JOURNAL OF SOLID STATE CHEMISTRY 74, 343–352 (1988)

$PbSn_4F_{10}$: A New Disordered Fluorite-Type Fast Ion Conductor

GEORGES DÉNÈS

Concordia University, Department of Chemistry and Laboratories for Inorganic Materials, Laboratory of Solid State Chemistry and Mössbauer Spectroscopy, 1455 de Maisonneuve Boulevard West, Montréal, Québec, Canada H3G 1M8

Received September 14, 1987

A new fluoride ion conductor, $PbSn_4F_{10}$, has been prepared in sealed copper tubes at 250°C, followed by quenching. It crystallizes in the fluorite structural type, space group $Fm3m$, with $a = 5.9541(5)$ Å, and exhibits total disorder between Pb and Sn. However, ^{119}Sn Mössbauer spectroscopy shows that the tin(II) lone pair has a $5s^{2-x}5p^x$ structure, and therefore is stereoactive with considerable p_z character. The Mössbauer parameters, $\delta = 3.38$ mm · sec^{-1} and $\Delta = 1.60$ mm · sec^{-1}, are very close to those for α-SnF_2, indicating a similar distortion of the tin(II) site, showing that despite the cubic symmetry of the lattice, the tin environment is probably similar to that observed in α-$PbSnF_4$. $PbSn_4F_{10}$ is metastable at room temperature and decomposes spontaneously over a period varying from a few minutes to a few days, depending on mechanical treatments. Promising fluoride ion conduction has been evidenced in this strange fluorite-type structure of SnF_2 stabilized with 20% PbF_2.

Introduction

Lead difluoride and stannous fluoride are both known for their polymorphism; α-PbF_2, stable at room temperature, crystallizes in the $PbCl_2$ type (space group = $Pmnb$, Pb coordination = 9) (*1*). It may be prepared by adding a soluble fluoride salt to a solution containing lead(II) ions. β-PbF_2, obtained upon heating the α-phase and stable indefinitely at room temperature upon cooling, is cubic, of fluorite (CaF_2) type (space group = $Fm3m$, Pb coordination = 8, regular cubic) (*2*). Stannous fluoride is known to crystallize in three polymorphs (*3*). Monoclinic α-SnF_2, stable form at room temperature, crystallizes from aqueous solutions (space group = $C2/c$, Sn coordination = Sn(1) = 3, Sn(2) = 5) (*4*). Tetragonal γ-SnF_2 is obtained at high temperature (space group = $P4_12_12$ or $P4_32_12$, Sn coordination = 4), and upon cooling to room temperature, it gives orthorhombic β-SnF_2 (space group = $P2_12_12_1$, Sn coordination = 4 + 1) (*5, 6*). The $\alpha \rightarrow \beta$ transition of PbF_2 and $\alpha \rightarrow \gamma$ transition of SnF_2 are characterized by their sluggishness, being spread over a wide temperature range, and are a function of factors such as grain size, mechanical treatments, and pressure (*3, 7, 8*). In both cases, a large hysteresis exists upon cooling and the high-temperature forms can be quenched to room temperature. However, β-SnF_2 converts back to the α-form in a few minutes to several days, whereas β-PbF_2 is indefinitely stable at room temperature. The $\beta \rightleftarrows \gamma$ transition of SnF_2 is a second-order ferroelastic–paraelastic transformation, and therefore presents no hysteresis.

The SnF_2/PbF_2 pseudobinary system was first studied by Donaldson and Senior (*9*),

0022-4596/88 $3.00

who isolated the compound $PbSnF_4$ from aqueous solutions upon addition of a hot saturated solution of lead(II) nitrate to an aqueous solution of tin(II) fluoride, which leads to immediate precipitation of tetragonal $PbSnF_4$ (space group $P4/nmm$). These results were confirmed by Dénès *et al.* in 1975 (*10*), who also prepared the isostructural $MSnF_4$ compounds (M = Pb, Sr, and Ba) in sealed gold tubes under dry nitrogen, at 250°C for $PbSnF_4$ and 550°C for $SrSnF_4$ and $BaSnF_4$. Donaldson and Senior (*9*) studied the SnF_2/PbF_2 system up to 60% PbF_2 by using transition-point data to plot the phase diagram upon cooling from the melt. The phase diagram shows three maximums for the crystallization temperature, at 80, 67, and 50 mole% SnF_2, respectively, which seem to indicate the existence of the following congruently melting compounds: $PbSn_4F_{10}$, $PbSn_2F_6$, and $PbSnF_4$, respectively. However, Donaldson and Senior were unable to isolate $PbSn_4F_{10}$ and $PbSn_2F_6$ and, as a consequence, assumed they were high-temperature phases.

We present in this paper the preparation and characterization of $PbSn_4F_{10}$. It is prepared by high-temperature reaction followed by rapid quenching. It is metastable at room temperature and decomposes in a few hours to give a complex mixture, confirming Donaldson and Senior's suspicion that it could exist as a high-temperature phase. Surprisingly, it crystallizes in the cubic fluorite-type structure with no apparent distortion; however, ^{119}Sn Mössbauer spectroscopy shows that the tin(II) environment is very irregular, and, therefore, that tin and lead are disordered on the metal site. Preliminary electrical conductivity measurements show that $PbSn_4F_{10}$ is a fluoride ion conductor as are SnF_2 (*11*), PbF_2 (*12*), $PbSnF_4$, and $BaSnF_4$ (*13*).

Experimental

Stannous fluoride, SnF_2, was a crystalline 99% purity product supplied by Omnium Scientifique Industriel, while powdered lead(II) fluoride 99.9%, PbF_2, was obtained from Alfa. The reagents were used without further purification. The appropriate stoichiometric mixture (SnF_2/PbF_2 = 4 : 1) was thoroughly mixed and ground in an agate mortar, then loaded in a copper tube sealed at one end. Temporary sealing of the second end was performed in a dry nitrogen glove box, which allowed final sealing to be done outside the glove box, while keeping the reagents under nitrogen. The tubes were heated at 250°C for periods of time varying from 1 to 4 hr then quenched by quickly immersing in cold water.

The melting point was measured using a standard Gallenkamp melting point apparatus calibrated *in situ* with α-SnF_2. ^{19}F NMR spectra were recorded on a Bruker W.H. 90 spectrometer operating at 84.669 MHz and were referenced against CCl_3F as zero chemical shift, negative shifts being to higher magnetic field strength. Differential scanning calorimetry (DSC) was performed using a Perkin–Elmer DSC-4 instrument, on 15.85 mg of sample contained in a platinum crucible, under a flow of dry nitrogen, at a heating/cooling rate of 10°C/min between RT and 300°C. Bulk density measurements were carried out at room temperature by displacement in carbon tetrachloride (Archimedean method). The powdered sample was evacuated on a high vacuum line (10^{-4} Torr) and immersed with CCl_4 while still under vacuum, in order to avoid trapping air bubbles between the particles. X-ray powder diffraction was carried out on a Philips PW1050-25 diffractometer, using the Ni-filtered $K\alpha$ radiation of copper (λ = 1.54178 Å). ^{119}Sn Mössbauer spectroscopy was performed using a $Ca^{119m}SnO_3$ 15-mCi γ-ray source purchased from Amersham. The Doppler velocity was obtained using an Elscint driving system working in the constant acceleration mode (triangular waveform). The γ-ray beam transmitted by the thin absorber was mea-

sured by a (Tl)NaI scintillation counter obtained from Harshaw. The spectra, recorded at room temperature, were accumulated in a 2K Tracor Northern 7200 multichannel analyzer operating in the multiscaling mode. After accumulation, the data were transferred to an IBM compatible personal computer and saved on a diskette. Computer fitting was performed on a CDC Cyber 835 main frame computer, using the GMFP5 software (*14*), which is a modified version of the GMFP program of Ruebenbauer and Birchall (*15*). The samples, 180 mg of powder, were pressed in a Teflon holder with a tightfitting cap. Isomer shifts were referenced to $CaSnO_3$ at room temperature as velocity zero.

Results and Discussion

The product, a white powder, was tested by powder X-ray diffraction. Table I gives the indexed powder pattern of $PbSn_4F_{10}$, and Table II gives some physical constants. The pattern is very simple and can be easily indexed in a cubic F lattice, identical to that of β-PbF_2. The unit cell parameter, refined from the powder data using the program PAFI of Le Marouille (*16*), is $a = 5.9541(5)$ Å, which is slightly larger than the value of 5.940 Å for β-PbF_2 (*2*) and corresponds to four-fifths molecule of $PbSn_4F_{10}$ per unit cell, i.e., four molecules of $Pb_{0.2}Sn_{0.8}F_2$ in the unit cell. The measured density of 5.449 g · cm^{-3} is in excellent agreement with the calculated value of 5.486 g · cm^{-3} (0.67% difference). The similarity with β-PbF_2, with a larger cell, may look surprising, as one would expect Sn(II) to be smaller than Pb(II), and, therefore, replacing 80% of lead(II) by tin(II) should result in a substantial decrease of the unit cell size, when going from β-PbF_2 to $Pb_{0.2}Sn_{0.8}F_2$, i.e., one-fifth of $PbSn_4F_{10}$. However, the contrary is observed. The identical powder diffracto-

TABLE I

$PbSn_4F_{10}$ X-RAY POWDER PATTERN

h k l	I/I_o	d_o (Å)	d_c (Å)	I/I_o (β-PbF_2)[a]
1 1 1	100	3.453	3.437	100
2 0 0	31	2.9765	2.9765	35
2 2 0	52	2.1071	2.1052	54
3 1 1	33	1.7952	1.7952	49
2 2 2	15	1.7199	1.7187	10
4 0 0	2	1.4877	1.4886	9
3 3 3 5 5 1	5	1.3658	1.3660	19
4 2 0	4	1.33098	1.33131	13
4 2 2	5	1.21532	1.21532	16
5 1 1	5	1.14581	1.14581	14
4 4 0	<1	1.05319	1.05251	5
5 3 1	1	1.00653	1.00638	14
4 4 2 6 0 0	1	0.992397	0.992397	7
6 2 0	<1	0.941575	0.941460	6
5 3 3	<1	0.907773	0.907991	5

[a] *Note.* The relative peak intensities for β-PbF_2 are given for comparison.

TABLE II

SOME PHYSICAL CONSTANTS FOR $PbSn_4F_{10}$

Cell parameter	$a = 5.9541(5)$ Å
Cell volume	$V = 211.1(3)$ Å^3
Space group	$Fm3m$–O_h^5 (No. 225)
Measured density	$\rho_o = 5.449$ g · cm^{-3}
Calculated density	$\rho_c = 5.486$ g · cm^{-3}
Density error	$\Delta\rho/\rho = -0.67\%$
Molecular weight	$M = 871.93$ g
Number of molecules $PbSn_4F_{10}$/unit cell	$Z = \frac{4}{5}$
Number of molecules $Pb_{0.2}Sn_{0.8}F_2$/unit cell	$Z' = 4$
Color	White
Melting point	272°C
^{119}Sn Chemical isomer shift[a]	$\delta = 3.45(1)$ mm · sec^{-1}
^{119}Sn Quadrupole splitting	$\Delta = 1.45(1)$ mm · sec^{-1}
Solubility in water at 20°C	0.525 g/100 cm^3 = 0.006 *M*
^{19}F Chemical shift[b]	$\delta = -91.4$ ppm
^{19}F Linewidth	$\Gamma = 20$ Hz

[a] Relative to $CaSnO_3$ at room temperature.

[b] On a saturated solution, relative to CCl_3F at room temperature.

gram for the two compounds and similar pattern in relative Bragg peak intensities (Table I) suggest that their structures are closely related. This point will be discussed in more detail below. If both compounds have a similar structure, it is unlikely that the substitution of a large amount of lead(II) by tin(II) would result in a less dense packing, sufficiently less dense as to reverse the sign of the volume change. In order to explain our results one must remember that ionic radii tables are based on the approximation that ions are spherical or close to spherical symmetry. However, Pb(II) and Sn(II) have a nonbonding electron pair (lone pair), which, when stereoactive, occupies one of the apexes of the polyhedron of coordination, which is very distorted (*17, 18*). Galy *et al.* (*18*) have shown that in such a case, the lone pair behaves, from the stereochemical point of view, as a ligand, and, therefore, the distance between the cation and its lone pair can be calculated. Using the data from a large number of known structures, it is found that, when going down a group of the periodical table, the larger the electronic core of an element, the shorter the distance between the cation and its lone pair. Therefore, the average M–E distance (E = lone pair) is 0.95 Å for Sn(II) and 0.86 Å for Pb(II), and as a result, the tin lone pair occupies a larger volume than the lead lone pair, which cancels the larger size of the lead atom for the divalent oxidation state. In addition, in β-PbF_2, the Pb(II) lone pair is not stereoactive. It results that the volume per MF_2 molecule is 53.3 Å^3 for α-SnF_2 (*4*) and 52.4 Å^3 for β-PbF_2; therefore, it is larger for α-SnF_2 than for β-PbF_2, and the value for $PbSn_4F_{10}$, equal to 52.8 Å^3, is intermediate, as one could have expected.

The powder pattern of $PbSn_4F_{10}$ being identical to that of β-PbF_2, with no superstructure Bragg peaks, indicates that tin and lead have to be disordered on the cation lattice. In the fluorite-type structure all atoms are in fixed positions of the $Fm3m$ space group, the metal in 0, 0, 0 (Wyckoff site 4a) and fluorine in $\frac{1}{4}, \frac{1}{4}, \frac{1}{4}$ and $\frac{3}{4}, \frac{3}{4}, \frac{3}{4}$ (Wyckoff site 8c), with the metal in cubic sites and the fluorine in tetrahedral coordination. Divalent tin usually does not take a regular coordination because of its stereoactive lone pair. No cubic coordination of tin(II) has been reported and only a few cases of regular octahedral coordination are known in compounds such as $CsSnX_3$ (X = Cl and Br) (*19*). This is possible because the tin(II) lone pair is on a $5s^2$ spherical orbital in these compounds. However, for fluorides, a $5s^{2-x}5p^x$ electronic structure is always encountered with considerable p_z contribution to the lone pair, and as a result, a highly distorted coordination of tin is observed. Therefore, it is highly unlikely that tin(II) is in a cubic environment of fluorine as Pb(II) in β-PbF_2. Crystallographic techniques give the long-range order between atoms, but they are of little help for the study of local distortion, whereas ^{119}Sn Mössbauer spectroscopy uses the ^{119}Sn nuclide for direct probing of the tin site. A regular cubic environment of tin would require the tin(II) valence electronic structure to be $5s^25p^0$, which would result in a very large isomer shift ($\delta \approx 4.0$ mm · sec^{-1}) and a zero quadrupole splitting due to the absence of electric field gradient (e.f.g.) at tin. The resulting Mössbauer spectrum would be a single line at a velocity close to 4.0 mm · sec^{-1}, as for cubic $CsSnCl_3$ and $CsSnBr_3$ (*19*). On the other hand, a stereoactive lone pair of electrons on tin(II), resulting in a distorted environment, requires a $5s^{2-x}5p^x$ tin(II) valence electronic structure. The $5p_z$ contribution to the lone pair creates a large e.f.g., $(V_{zz})_{val}$, resulting in a large quadruple splitting. The lattice component of the e.f.g., $(V_{zz})_{lat}$, originates at the highly disturbed coordination of tin; however, this is usually a minor component (*20*). The observed Mössbauer spectrum for $PbSn_4F_{10}$ (Fig. 1) shows the characteristic doublet as

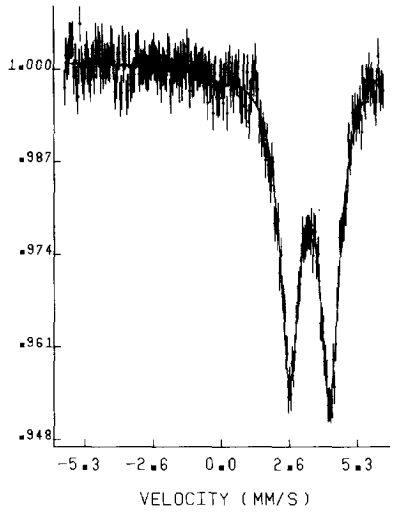

FIG. 1. ^{119}Sn Mössbauer spectrum of $PbSn_4F_{10}$ at room temperature.

for α-SnF_2 (*21*), $PbSnF_4$ (*22*), and $BaSnF_4$ (*13*). The isomer shift and quadrupole splitting values given in Table II give an unambiguous proof that there is considerable p_z character in the lone pair, and, therefore, the tin environment is strongly distorted. The doublet asymmetry most likely arises from: (i) texture effect as preferred orientation is very often encountered in lone pair compounds because of easy directions of cleavage (*22*), and (ii) the Goldanskii–Karyagin effect due to tin thermal vibration anisotropy; both cases (i) and (ii) originate in the tin bonding anisotropy due to repulsions between tin lone pairs, and their effect can add up or partly cancel each other, depending on the case. The small tin(IV) line at ca. 0 mm · sec^{-1} is a tin(IV) impurity, which is also found in the powdered α-SnF_2 used for the synthesis. It is due to surface oxidation of the crystallites, giving SnO_2. As the recoil-free fraction of SnO_2 is more than 10 times as high as that for tin(II) fluorides (*22, 23*), and the Sn(IV) signal is ca. 2% of the total signal, the SnO_2 content in the sample is estimated to be smaller than 0.2%.

The β-PbF_2 fluorite-type structure is made of a three-dimensional network of cubes of fluorine atoms, half of which are occupied by lead, such that filled and empty cubes alternate along directions parallel to the three axes of the cubic cell (Fig. 2a). In β-PbF_2, lead occupies exactly the center of half of the fluorine cubes, and therefore, has a cubic coordination (Fig. 2b). Divalent tin cannot take this type of coordination as

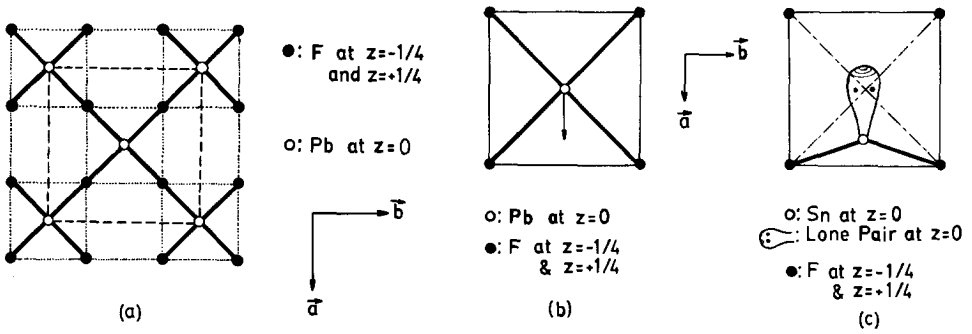

FIG. 2. (a) Three-dimensional network of empty and occupied cubes of fluorine atoms in β-PbF_2. The dotted lines (· · ·) indicate the network of fluorine cubes, the dashed lines (- - -) show the cubic unit cell of β-PbF_2, and the solid lines (—) represent the Pb–F bonds. (b) A cube of fluorine atoms with a Pb occupying its center. The arrows indicate the metal shift out of the center of the cube when replacing Pb by Sn in $PbSn_4F_{10}$. (c) Tin(II) in square pyramidal coordination in $PbSn_4F_{10}$. The lone pair is located close to the center of the cube.

shown by Mössbauer spectroscopy. In order to fit a stannous tin with its lone pair inside a fluorine cube, tin must be displaced out of the center of the cube. Figure 2c shows the most probable configuration, which consists of moving tin along one of the fourfold axes of the cube, i.e., tin being in $x\,0\,0$ (Wyckoff site 24e of the space group $Fm3m$) with the occupancy factor of 0.1333 [i.e., $4 \times (\frac{1}{24})$ of 0.8]. There are six ways of shifting each Sn, i.e., toward each face of the cube. In this model, Pb stays in the 4a site with an occupancy factor of 0.2, and F is located in site 8c with an occupancy factor of 1.0, as in β-PbF_2. Tin and lead are obviously disordered, as order would necessarily result in a supercell, probably of lower symmetry. For example, we have proposed a similar displacement of tin in β-$PbSnF_4$; however, in this case, Pb and Sn are ordered (*24, 25*), giving rise to a tetragonal distortion and a supercell of β-PbF_2. In this model, tin in a square pyramidal coordination similar to that observed in black SnO (*26*). The bonding and anion–lone pair repulsions in SnO and in our model of $PbSn_4F_{10}$ are compared in Fig. 3. Figure 3a shows the SnO structure with four equal SnO distances of 2.22 Å. Using the average tin(II)–lone pair distance of 0.95 Å determined by Galy *et al.* (*18*), one finds four equal distances of 3.33 Å between the lone pair and the nearest oxygen atoms, which is much larger than the minimum oxygen–oxygen distance of 2.84 Å found in ionic solids, determined from the radius of 1.42 Å for O^{2-}, according to Shannon and Prewit (*27*). It results in weaker interlayer repulsions than expected for this layered structure, which is probably responsible for the small thermal expansion coefficient along **c** (*26*). A similar calculation for $PbSn_4F_{10}$, using the ionic radius for F^- equal to 1.33 Å (*27*), gives Sn–F distances of 2.13 Å and fluorine–lone pair distances of 2.71 Å (minimum F–F distance = 2.66 Å) for the fluorine atoms not bonded to that tin. However, the distances between the lone pair and the fluorine coordinating tin are equal to 2.46 Å, which is clearly too short. The model is improved by placing the lone pair at the center of the fluorine cube, which gives d(Sn–F) = 2.58 Å for the eight fluorine atoms surrounding the lone pair, which is close to the estimated minimum of 2.66 Å. In this case, still for a Sn–E distance of 0.95 Å, the Sn–F distances are 2.17 Å, which are commonly encountered Sn(II)–F bonding distances. Therefore, the above model, suggested by X-ray diffraction and

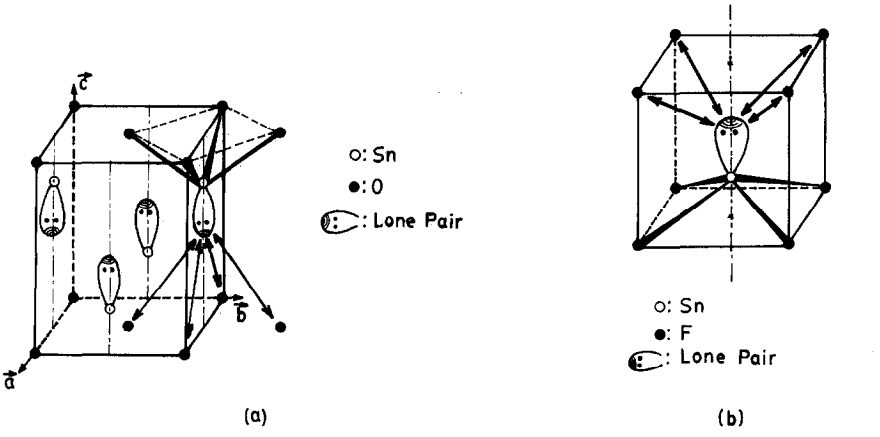

FIG. 3. Square pyramidal coordination of Sn(II) and lone-pair anion repulsions in (a) black SnO; (b) $PbSn_4F_{10}$. Lone-pair anion repulsions are indicated by double arrows (↔).

Mössbauer spectroscopy, is very reasonable from a simple crystal chemistry point of view.

$PbSn_4F_{10}$ is not very stable and spontaneously decomposes at room temperature, over a time varying from a few hours to several days. Decomposition is greatly accelerated upon grinding, i.e., by application of mechanical energy. As $PbSn_4F_{10}$ is obtained only upon quenching, it is clear that it is a high-temperature form, which confirms the suspicion of Donaldson and Senior (*9*), originating from the observation of a melting temperature maximum at 80 mole% Sn in the SnF_2/PbF_2 system; thus $PbSn_4F_{10}$ is stable only at high temperature and melts congruently, but it can exist in a metastable state at room temperature for a short period of time. Pannetier and Dénès (*26*) attributed the unusually low thermal stability and high reactivity of SnO to the large O–Sn–O angles of 117°. In the above structural model of $PbSn_4F_{10}$, the F–Sn–F angles are 87° for adjacent fluorines, which are commonly encountered values, but the angles between diagonal fluorines are 152°, i.e., much larger than the values observed in SnO. However, for the equatorial fluorine atoms of Sn(2) in α-SnF_2 (*4*) and in $BaSnF_4$ (*25*), which have a related coordination of tin with, in addition, a short axial Sn–F bond perpendicular to the plane of the equatorial fluorine, i.e., coaxial to the Sn–*E* axis but on the opposite side of Sn, similar angles are found; but, the axial fluorine is responsible for pulling tin toward the equatorial fluorine plane in those structures. Therefore, the unusually large bond angles and tight fitting of tin and its lone pair in the fluorine cubes may be responsible for the low stability of $PbSn_4F_{10}$ at room temperature. We have considered here that the fluorine positions are identical for PbF_8 and SnF_8 cubes; however, it is possible that the fluorine atoms shift to allow a more comfortable site for Sn and the lone pair. Although this would increase the stability at the tin site, it would destabilize the lead sites for the leads in adjacent cubes, which would be forced by tin to accommodate to a distorted site. In addition, fluorine shifts would also have to be disordered because there is no superstructure or symmetry break.

Conclusion

The compound $PbSn_4F_{10}$, whose existence was suspected, based on solidification experiments in the PbF_2/SnF_2 phase diagram, has been prepared and characterized. It is a high-temperature phase, but we have been successful in keeping it in a metastable state at room temperature upon quenching. Decomposition occurs in as short as a few minutes in some cases, but can take several hours or 2 to 3 days in other cases. The poor stability of the compound can be attributed to its crystal structure, because (i) tin(II) and its lone pair are located in cubes of fluorine atoms, which are slightly too small, resulting in a too tight fitting, (ii) there are unusually large F–Sn–F angles for a square pyramidal coordination, and (iii) there are strong fluorine–lone pair repulsions. The products of decomposition are a complex mixture in which we could identify α-SnF_2, α-$PbSnF_4$, and a large number of other peaks we could not assign to any known compound. If the compound $PbSn_2F_6$, also predicted by Donaldson and Senior (*9*) from solidification curves, exists, it should be one of the products of decomposition instead of $PbSnF_4$. However, as $PbSn_2F_6$, if it exists, is probably also a high-temperature phase and therefore would decompose at room temperature to give α-SnF_2 and α-$PbSnF_4$ as well, $PbSnF_4$ is obtained instead of $PbSn_2F_6$. We have tried to isolate $PbSn_2F_6$ upon quenching; however, the product obtained was always a very complex mixture similar to the products of decomposition of $PbSn_4F_{10}$, i.e., containing α-SnF_2, α-$PbSnF_4$, and

a large number of unidentified peaks, some of which are also observed upon decomposition of $PbSn_4F_{10}$. Therefore, we can conclude that $PbSn_2F_6$ probably also exists at high temperature, but it is even more unstable than $PbSn_4F_{10}$.

It is very strange that $PbSn_4F_{10}$ crystallizes in an undistorted β-PbF_2 structural type with total absence of long-range order between tin and lead. Although tin(II) and lead(II) are randomly disordered on the metal site, ^{119}Sn Mössbauer spectroscopy shows that the tin environment is not cubic as Pb(II) and has a stereoactive lone pair of electrons with considerable p_z character. It is very surprising that such a highly symmetrical structure, characteristic of MF_2, with M in cubic coordination, can be formed when only 20% of the metal takes the cubic coordination such that $PbSn_4F_{10}$ can be considered as a high-temperature fluorite form of SnF_2, stabilized by 20% PbF_2 impurity. It is even more surprising that this occurs only for the exact composition $Pb_{0.2}Sn_{0.8}F_2$. There is no solid solution as slight deviations from the exact Pb/Sn = 1 : 4 stoichiometry resulted in excess SnF_2 or $PbSnF_4$ being obtained. We hope to learn more about this strange compound, which really does not make sense from a crystal chemistry point of view, using neutron powder diffraction.

The melting point of 272°C, observed using a melting point apparatus is higher than that of α-SnF_2, 215°C (*3*), and much lower than that of PbF_2, 855°C (*28*), as could be expected. The heating and cooling DSC curves from RT to 300°C are shown in Fig. 4. Upon heating (Fig. 4a) a series of three or four overlapping endothermic peaks are observed between 190 and 210°C and a sudden baseline change starting at ca. 280°C (or a very broad event extending from ca. 200 to 280°C), which is probably melting as we observed it to occur at 272°C, although it is not shaped like a melting peak. The endothermic events at 190–210°C are probably

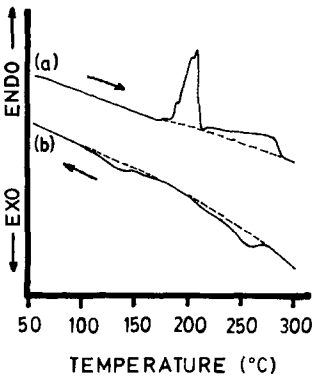

FIG. 4. DSC curve of $PbSn_4F_{10}$: (a) heating, (b) cooling.

due to the melting of SnF_2 enriched in lead and the reaction between the decomposition products giving back $PbSn_4F_{10}$, as the sample was 3 days old when the DSC experiment was performed, and, therefore, mostly decomposed as shown by a subsequent X-ray powder pattern. The cooling curve (Fig. 4b) shows a broad exothermic event starting at ca. 270°C and extending to about 200°C, corresponding to solidification of the melt, which occurs with a few degrees hysteresis, a phenomenon not unheard of for tin(II) fluorides as solidification of SnF_2 can occur with as much as 30°C hysteresis (*3*). The peaks observed at around 200°C upon heating are not observed upon cooling (as the mixture responsible for them no longer exists), showing they were not the melting of $PbSn_4F_{10}$. On cooling, a very broad endothermic peak from ca. 170 to about 100°C is obtained. This can be attributed to the slow decomposition of $PbSn_4F_{10}$ as X-ray diffraction shows $PbSn_4F_{10}$ can be isolated at room temperature only if fast quenching is performed.

The fluorite-type lattice of $PbSn_4F_{10}$ is not readily broken apart by water as the solubility in water at 20°C is ca. 0.525 g in 100 cm^3, i.e., a saturated solution has a concentration of 0.006 M $PbSn_4F_{10}$, i.e., 0.030

M $Pb_{0.2}Sn_{0.8}F_2$. This compares well with the low solubility of PbF_2 (0.026 *M*) (*28*) and contrasts with the high solubility of α-SnF_2 (3.9 *M*) (*29*) and indicates that the lattice type is the preponderant factor over chemical composition for the stability of the crystalline lattice against solvent destructive action. A very small amount of $PbSn_4F_{10}$ did not dissolve, even for much larger dilutions, but this was too small to be collected for identification. ^{19}F NMR spectroscopy of the saturated solution gave a single line, fairly broad (20 Hz), at $\delta = -91.4$ ppm chemical shift relative to CCl_3F, which is characteristic of $SnF_2 \cdot H_2O$ as shown by Birchall and Dénès (*29*). As in (*29*), absence of coupling to $^{117,119}Sn$ and the fairly large linewidth indicate that a slow ligand-exchange process is taking place. It is likely that the equation of dissolution is the following:

$$PbSn_4F_{10} + 4H_2O \xrightarrow{H_2O} \underset{\downarrow}{PbF_2} + 4SnF_2 \cdot H_2O. \quad (1)$$

^{119}Sn Mössbauer spectroscopy also shows, as tin(II) in $PbSn_4F_{10}$ has a $5s^{2-x}5p^x$ valence electronic structure, the band gap is too high to give rise to semiconducting properties. Therefore, the compound is an insulator, unless ionic conductivity is present, due to long-range motion of fluoride ions, a very likely situation in a fluorite-type structure containing divalent tin (*13*). Preliminary electrical conductivity measurements have shown that $PbSn_4F_{10}$ is indeed a good ionic conductor. A detailed study of its conducting properties is under investigation.

Acknowledgments

Concordia University and the Programme d'Actions Structurantes of Québec are gratefully acknowledged for financial support. Technical support from Concordia University Scientific Shop is acknowledged. The Natural Science and Engineering Research Council of Canada is thanked for a University Research Fellowship. I am indebted to Dr. M. F. Bell (Concordia University, Montréal, Québec) and Professor M. Sayer (Queen's University, Kingston, Ontario) for their help in the preliminary electrical conductivity measurements. Mr. B. G. Sayer (McMaster University, Hamilton, Ontario) is thanked for the NMR measurements. We are grateful to Mr. P. Toma (Pharmaceutical Research Division, Merck-Frost Canada Inc., Montréal, Québec) for the DSC experiment.

References

1. R. W. G. Wyckoff, "Crystal Structures," 2nd ed., Vol. 1, p. 300, Interscience, New York (1963).
2. A. R. West, "Solid State Chemistry and its Applications," p. 240, Wiley, New York (1984).
3. G. Dénès, *Mater. Res. Bull.* **15,** 807 (1980).
4. G. Dénès, J. Pannetier, J. Lucas, and J. Y. Le Marouille, *J. Solid State Chem.* **30,** 335 (1979).
5. G. Dénès, J. Pannetier, and J. Lucas, *J. Solid State Chem.* **33,** 1 (1980).
6. J. Pannetier, G. Dénès, M. Durand, and J. L. Buevoz, *J. Phys.* **41,** 1019 (1980).
7. G. Dénès, *J. Solid State Chem.* **37,** 16 (1981).
8. V. K. Mahajan, P. T. Chang, and J. L. Margrave, *High Temp.–High Pressures* **7,** 325 (1975).
9. J. D. Donaldson and B. J. Senior, *J. Chem. Soc. A,* 1821 (1967).
10. G. Dénès, J. Pannetier, and J. Lucas, *C.R. Acad. Sci. Paris Ser. C* **280,** 831 (1975).
11. D. Ansel, J. Debuigne, G. Dénès, J. Pannetier, and J. Lucas, *Ber. Bunsenges. Phys. Chem.* **82,** 376 (1978).
12. J. H. Kennedy, R. Miles, and J. Hunter, *J. Electrochem. Soc.* **120,** 1441 (1973).
13. G. Dénès, T. Birchall, M. Sayer, and M. F. Bell, *Solid State Ionics* **13,** 213 (1984).
14. J. Monnier, G. Dénès, and R. B. Anderson, *Canad. J. Chem. Eng.* **62,** 419 (1984).
15. K. Ruebenbauer and T. Birchall, *Hyperfine Interact.* **7,** 125 (1979).
16. J. Y. Le Marouille, Thèse de 3ième cycle, Université de Rennes I, Rennes (1972).
17. I. D. Brown, *J. Solid State Chem.* **11,** 214 (1974).
18. J. Galy, G. Meunier, S. Andersson, and A. Aström, *J. Solid State Chem.* **13,** 142 (1975).
19. J. D. Donaldson and J. Silver, *J. Chem. Soc., Dalton. Trans.,* 666 (1973).
20. J. D. Donaldson, D. C. Puxley, and M. J. Tricker, *Inorg. Nucl. Chem. Lett.* **8,** 845 (1972).
21. T. Birchall, G. Dénès, K. Ruebenbauer, and J. Pannetier, *J. Chem. Soc., Dalton Trans.,* 1831 (1981).
22. T. Birchall, G. Dénès, K. Ruebenbauer, and

J. PANNETIER, *J. Chem. Soc., Dalton Trans.*, 2296 (1981).

23. V. A. BRYUKHANOV, N. N. DELYAGIN, A. A. OPALENKO, AND V. S. SHPINEL, *Sov. Phys. JETP* **16,** 310 (1963) [*J. Exp. Theor. Phys. (U.S.S.R.)* **43,** 432 (1962).]
24. J. PANNETIER, G. DÉNÈS, AND J. LUCAS, *Mater. Res. Bull.* **14,** 627 (1979).
25. T. BIRCHALL, G. DÉNÈS, K. RUEBENBAUER, AND J. PANNETIER, submitted for publication.
26. J. PANNETIER AND G. DÉNÈS, *Acta Crystallogr. Sect. B* **36,** 2763 (1980).
27. R. D. SHANNON AND C. T. PREWITT, *Acta Cyrstallogr. Sect. B* **25,** 925 (1969).
28. R. C. WEAST, Ed., "CRC Handbook of Chemistry and Physics," 61st ed., p. B-111, CRC Press, Boca Raton, FL (1980–1981).
29. T. BIRCHALL AND G. DÉNÈS, *Canad. J. Chem.* **62,** 591 (1984).